Global Transitions Proceedings 2 (2021) 392–401

Contents lists available at ScienceDirect

Global Transitions Proceedings

journal homepage: http://www.keaipublishing.com/en/journals/global-transitions-proceedings/

A review on remote health monitoring sensors and their filtering techniques

Divya Sri Rajeswari*, Hitha Shree J, Ananya L.N. Simha, Maria Nuzhath Subhani, Shivaleelavathi B G, Veeramma Yatnalli

JSS Academy of Technical Education, Dr. Vishnuvardhan Rd Uttarahalli-Kengeri Main Road, Srinivaspura, Bengaluru 560060, India

ARTICLE INFO

Keywords:
COVID-19
ECG monitoring
Health monitoring
Lung acoustic signals
Machine learning
MIT-BIH arrhythmia database
Pan-Tompkins algorithm
Pulse oximetry
QRS complex
Temperature sensor

ABSTRACT

The novel coronavirus outbreak has affected over 177 million people in around 218 countries and Territories. Covid-19 is life-threatening for the elderly and for those with chronic health conditions. This has set out a state of panic where people have the need to constantly monitor their health. The objective of this paper is to review the various sensor components, filtering algorithms, classification techniques, existing methods and technologies that play an important role in developing a safe remote health monitoring device. Comparison of sensor devices is done to understand the features of available products in the market. An extensive survey of ECG monitoring, lung acoustic signals and how COVID-19 affects this vital signature, thermal sensors, and pulse oximeters are presented. The need for a device in this situation to cater to the health issues is necessary.

1. Introduction

Globally, COVID-19 accounts for more than 177 million cases with more than 3.8 million deaths. India currently has the largest number of confirmed cases in Asia with more than 29 million reported cases. And over 300 thousand deaths. Considering the current situation in India, there are almost 50 thousand people who are getting affected by COVID-19 every day, as per the statistics. Infection rate is increasing day by day which is mainly affecting people with medical history, old aged and children. The fatality rate is around 2.41% which is among the lowest in the world. Symptoms can be mere or severe, as per the observations, the initial symptoms of COVID-19 include fever, cold, fatigue, cough, loss of smell and taste. When these symptoms are left unnoticed, they can become severe causing pulmonary problems (like pneumonia and acute respiratory distress syndrome) which might lead to death. The abnormalities in the respiratory system have a major impact on the heart. Since the heart requires ample amounts of oxygen for its functioning, deficient amounts of it can lead to life-threatening events like Ventricular fibrillation, Angina, Arrhythmias as well as minor events like gastrointestinal disorder.

Though COVID-19 is considered as acute respiratory syndrome it has its major drawback on old aged people with 60+ years or with health conditions like lung or heart disease, diabetes or conditions that affect the immune system, this includes children below 5 years. During this pandemic it is very essential for one to know the importance of health. The angst of COVID has drawn people to depression making them more anxious. As a result, people fail to have track of their health. Since anxiety is one of the key factors of Arrhythmia, it is very important to remain calm and have proper balance on physical exercise and mental health. It is necessary to have a regular check on our vital values, in case of any discrepancy one can get medical attention well in advance to avoid the catastrophe.

To monitor these values there are many health monitoring systems developed like smart watches and wear bands which monitors and displays the real-time values. The recent innovation on these have tracked on heart rate, body temperature, calories burnt, distance covered which are mostly used for fitness tracking. Though they are very efficient it lacks an alert system and also, they fail to account for lung sounds and capacity as it is considered the most crucial criteria for the diagnosis of COVID-19.

2. Related works

A wearable, continuous ECG and an acoustic monitor [1] that detects any abnormalities in the chest and provides actionable advice to the user in real-time. The user's temperature and oxygen saturation level in the blood is not considered. These vital values will be crucial to determine the overall user health. Extended monitoring of arrhythmias in real-world settings is conducted using ambulatory ECG devices. The design flow, functionality, indications, efficacy, cost, and optimal use of these devices are discussed in [2]. The paper lacks to discuss patient monitoring outside the ambulance. No other vital other than the patient ECG is monitored. There is no alert system in case of a medical emer-

* Corresponding author.
E-mail address: divyarac@gmail.com (D.S. Rajeswari).

https://doi.org/10.1016/j.gltp.2021.08.022
Received 19 May 2021; Accepted 28 June 2021
Available online 12 August 2021

gency. The paper [3] gives a review and analysis to help the detection of abnormal lung sounds for specific respiratory disorders by discussing the implementation of computerized lung sound analysis (CLSA). Since no patient health is tracked, the data is not collected in real-time. The designed technique may not work with smart wearables.

An ECG based monitoring system for heart abnormality detection using wearable sensors is analyzed in [4]. It also discusses devices based on PPG signals that are non-invasive and portable. The system does not account for any respiratory monitoring. Shortness of breath is one of the main symptoms for heat-related illnesses, which is not considered in the paper. The authors in [5], review the probable mechanisms that could result in arrhythmogenesis among COVID-19 patients which includes a condition of hypoxia due to direct viral tissue involvement of lungs, myocarditis, abnormal host immune response, myocardial ischemia, myocardial strain, electrolyte derangements, imbalances in intravascular volume, and sides effects of various drugs which are ingested. To supervise these arrhythmias, it is highly important to be aware of the potential drug-to-drug interactions, to observe QTc prolongation while receiving treatment and also provide special attention for patients with inherited arrhythmia syndromes. It is also imperative to minimize the risk of infection exposure by classifying the need for intervention and by employing telemedicine.

The paper [6] talks about the future of biomedical sensors where patient's physiological or biochemical parameters can be tracked in real time under any environment. The sensors with the apps can collect the real time data and interpret, and can be stored in cloud, the network of sensors and body networks will make healthcare's Internet of Things. In this analysis, four important areas of attentiveness for respiratory healthcare are described: pulse oximetry, pulmonary ventilation, activity tracking and air quality assessment. This wearable does not monitor the ECG signals, which is the most important criteria to be considered for heart abnormality detection. In the journal article [7], the Deep learning algorithm 'nCovnet', developed uses X-ray images from an open-source data set by Cohen at al. Posterior Anterior (PA) feature is selected to differentiate COVID-19 positive and negative patients by using the VGG16 model for feature extraction as a base model. It achieved a 97.62% true positive rate. The Deep Learning model is trained and tested only on COVID 19 positive patients' X-ray images and X-ray images of non-COVID 19 patients' is not taken into consideration.

The impact of [8] implies that the MIT-BIH arrhythmia database is an open dataset which acts as a standard investigation material for the detection of heart arrhythmia. It consists of 48 half-hour excerpts of two-channel ambulatory ECG recordings, recorded from 47 subjects, studied at the BIH Arrhythmia Laboratory during 1975–1979. Variations in recording and playback speed need to be considered carefully for heart-rate variability studies since flutter compensation was not possible during recordings. In [9], a three-lead electrocardiogram acquisition system is assembled with an analog front-end circuit, a microprocessor and the ECG data is displayed using a MATLAB simulator and stored on the cloud. Here the major drawback is that the wavelet algorithm and noise cancellation methodologies are not explained in detail. Paper [10] compares the classification of respiratory sounds using both artificial neural networks (ANNs) and adaptive neuro-fuzzy inference systems (ANFIS) toolboxes. Autocorrelation function is utilized in feature extraction which enhances the performance, acquiring accuracy of 98.6%. But abnormal respiration cannot be concluded as deterioration of health. Data set of patients diagnosed with other respiratory problems are not considered.

The paper [11] centralized on the execution of an algorithm which is able to recognize the noise which can be classified as either voluntary or involuntary produced during the acquisition of lung sound. As of now there are no algorithms to sense the noises in the lung sounds which includes the vocal sounds and/or other disturbances from the environment. The required algorithms should be able to recognize the cough, cough period as one of the symptoms to detect the pulmonary abnormalities. This paper [12] gives a brief about a variety of wearable sensors that have attracted due to its potential of acquiring real time values and processing it through various non-invasive methods. Several commercially non-invasive and minimally invasive biosensors are compared. The paper reviews: Biosensor components, the path of biosensor development, epidermal iontophoretic biosensors, epidermal biosensors for real-time monitoring of sweat chemistry, Oral-cavity wearable biosensors, and Tear-based biosensors.

In the article, [13] it is seen how wearable technology can help the patients who are affected with COVID-19 by providing real time values and continuously keeping in track of the symptoms. This paper briefs about the suitable wearable technology which assists to battle against the current situation. This entire process can be categorized into two stages: one for keeping in track of the initial conditions of COVID-19, and other to monitor the pulmonary abnormalities in the infected patients. Due to complexity in sensor hardware technology, it is quite tedious to check the symptoms and process it in one combined module. More work should be carried out on monitoring systems with much higher sensitivity so that early detection can be achieved.

2.1. Literature survey on sensors and algorithms

The authors in [14] review an ECG signal analysis system to measure rhythm and regularity of the heartbeat. It tells how the ECG signals are obtained, its waveform, Cardiac diseases detected by ECG, Arrhythmia and the extraction of the ECG Signals. It further explains the methods of classifying a signal into normal, arrhythmia and ECG signals. However, this paper does not give an insight into the working of the ECG machine or the various algorithms used to get rid of the noise to get a clear signal. Paper [15] proposes a new method to extract ECG signal features. The analysis to detect normal and abnormal heart rate is reviewed. It discusses the various parameters of classifying a signal. It aims at building an efficient algorithm to detect the functioning of the heart. It does not talk about the ECG monitoring Architecture and its comparative study, the key challenges and Technology aware ECG monitoring. The paper, [16] proposes an ECG front-end signal processing technique that is used to reduce noise interferences in ECG signals. This technique implements Radio-Frequency Interference (RFI) filter, a type of bridge differential low-pass filter with a high precision instrument input amplifier AD8220. The Bessel filter and right leg driving circuit make up the low-pass filter stage. The focus is on the easy integration, good stability, high accuracy, high precision, and simple signal processing of ECG front-end devices.

Paper [17] gives a brief information on the properties of lung acoustic signals during normal breathing. There are two types of lung sounds: tracheobronchial and vesicular lung sounds. A modern method of auscultation of lung sounds using different sensors, processing of raw data and analysis of the physiological data. The article, [18] showcases the importance of air cavity, width and shape of the chamber of the coupler as it has an impact on the lung acoustic signals. The journal article [19] compares the sensors used in the acquisition of lung sounds, it compares the two types of microphones used: air-coupled and contact sensors. Comparison is done based on dimensions as well as based on the power spectral analysis. Article [20] gives detailed information on the types of lung sounds, their characteristics, properties which include frequency, intensity and quality of lung sounds. The mechanism of breath sounds is also explained in brief.

The article [21] presents a classic method of processing lung sound is to filter the obtained acoustic signals using high-pass filter with cut-off frequency from 50 to 150 Hz. Since the range of lung sound is about 20–1600 Hz, a single high pass filter is used. However, this produces distortion, hence to attain better results on de-noising there are two ways: wavelet shrinkage de-noising and adaptive filtering algorithm. The former method is based on the wavelet packet, which reduces the noise without disturbing the original lung acoustic signal. The latter one is used to eliminate heart sound from the lung sound using adaptive filters on the obtained lung sound with second order Auto regressive process. In this paper [22], Spectro-temporal representation is used to enhance

the separation of heart sound and lung sound. The band pass and band stop filters are used to distinguish the heart sounds, and lung sound is the obtained lung acoustic signal. Along with visual and auditory study, quantitative study is also performed on the obtained model. In [23], another de-noising method is used to differentiate lung sound and other sounds, and filter out the noise retaining the lung sound using Savitzky-Golay filter. The signal to noise ratio provides the frame length and order of the filter.

The research paper [24] illustrates the effect caused by lung sounds due to COVID-19, the abnormalities in the lung sounds. The pulmonary details of two infected patients are examined and the effect of COVID-19 on the pulmonary system is being highlighted. Journal [25] provides the pathological examination of infected patients and the obtained results are being compared with the normal/uninfected candidate vital readings. The various stages of the diagnosed people are considered to have a thorough analysis of the present pandemic COVID-19. The patent, [26] presents an innovative low-cost temperature sensor consisting of a thermistor that is surface-mounted in a circuit. It is a highly responsive component that has three layers of electrical circuit substrate which is in thermal coupling to a metal base layer situated on the opposite side. The intermediate layer is made up of an electrically insulated material that secures the base layer and the conducting metal layers. Replacement of costly wires and lead-frames are part of the flexible circuit technology that is incorporated in this [27] temperature sensor. Paper [28] emphasizes on the importance of remote health monitoring and aims to design a body temperature measurement device. This device also stores the data history of the user using Xbee wireless technology, which can be monitored by the doctor in real-time. An Arduino with IEEE 802.11 based Ethernet shield is used to send the real-time data to a database. These body temperature results are compared with that taken from a commercial thermometer. A system that is capable of monitoring the heart rate and body temperature remotely is designed in [29]. A team of researchers have collected the data from volunteers using this developed sensor system. The collected data is transmitted to a remote PC station using an Arduino microcontroller and an XBee wireless network.

The authors [30] demonstrate a Transparent Stretchable (TS) dated sensor array that is capable of high stretch ability of 70%. This wearable temperature sensor has high optical transparency and conformity. It has a high response rate to changes in temperature in human skin and objects. The device poses a potential application to the new era of wearable electronics. Respiratory status is monitored using Pulse oximetry [31], and for critically ill patients, pulse oximetry monitoring is very important. The performance of pulse oximeters has improved from the advancement in the domains of signal analysis and reflectance technology. Paper [32] introduces a medical system that is used for monitoring patient health. This wireless interface of infrastructure uses Bluetooth sensors, WLAN and GPRS to transmit the recorded pulse-oximetry signals. The authors in [33] review the non-invasive nature of pulse oximeters and its importance in evaluating the respiratory system. Commercially available pulse oximeters possess an error rate of 3–4%.

The performance of four motion-resistant pulse oximeters is compared and present in [34]. It is found that the motion and low perfusion had an impact on the pulse oximeters. It degraded the performance of the pulse oximeters, although all the types detected hypoxia with a specificity of 95% or higher. The study, [35] indicated that pulse oximeter probes that are attached to the earlobe show a higher accuracy in SpO2 readings among intensive care unit patients when compared to the probes that were attached to the toe, finger and forehead. The article, [36] discusses the real-time approach of this algorithm and gives a vast and detailed insight into the numerous filters and learning models used. It has an efficiency rate of 99.3% on a standard MIT Arrhythmia dataset and also has the advantage of increasing the sensitivity of detection by using lower threshold values. This has an edge over other algorithms as it adapts to ECG changes like QRS morphology and heart rate. The only drawback is that this algorithm was implemented in Z80 assembly language. (But is now available in MATLAB and can be incorporated in other high-level programming languages). The conference paper, [37] inspects the performance of the Pan-Tompkins algorithm with low-quality noisy ECG signals with different Signal-to-noise ratios (SNR). For the two datasets used-NST and MIT, the algorithm proved efficient with detection sensitivity greater than 90% with SNR ranging from 24 to 6dB. However, with strong noise signals such as SNR -6dB, the performance of the algorithm was compromised. Research paper [38] gives a comparative study of ten commonly used QRS detectors. This paper gives clarity on different algorithms' reliability and efficiency. Even though the Optimized Knowledge-Based (OKB) algorithm appears to be the most efficient algorithm followed by the P.T algorithm, it is very difficult to be implemented. Hence the P.T algorithm is most commonly used. Paper [39] is also a comparative analysis of the three most commonly implemented algorithms- Pan Tompkins, Hamilton Tompkins and Phasor Transform, over a public database. It gives a clear result that the P.T algorithm is better and the results are tabulated in Table 1, which is taken from the above-mentioned paper.

Table 1
Mean results for each algorithm over database records [39].

Algorithm	Sensitivity	Pos. Productivity	RMS RR Error
Pan & Tompkins	99.79% ± 0.34	99.84% ± 0.42	95.88 ms
Hamilton & Tompkins	99.54% ± 0.69	99.42% ± 1.19	107.03 ms
Phasor	98.41% ± 4.95	86.75% ± 17.30	354.84 ms

In the paper, [40], the performance of Support Vector Machine (SVM) algorithm was assessed against the standard CSE ECG database. The results showed a staggering detection efficiency of 99.3% for the given algorithm. Even with an abysmal quality of ECG signals, the reliability of the algorithm was high. As only a single lead ECG data were considered, the false percentage was more. On employing 3 lead or 12 lead ECG data the false rate decreases exponentially. In the journal, [41], the authors explore the SVM classifier for QRS complex detection. Classification was based on the standard MIT-BIH arrhythmia database. The results indicated a 99.87% efficiency for the algorithm. This classifier performs better with respect to other classifiers for the same database. In [42], the authors achieve a higher efficiency and accuracy rate using SVM classifier by reducing the features using the Gaussian Discriminant Analysis (GDA) algorithm. The article, [43] gives the clear efficiency difference of SVM classifier and k-nearest neighbors (KNN) classifier for QRS complex detection for various models in Figs. 1 and 2, which are taken from the above-mentioned paper.

Various hardware and software technologies are used to implement the remote health monitoring system. A set of biosensors and filtering algorithms are discussed as per the taxonomy of research shown in Fig. 3.

2.1.1. ECG

ECG or EKG (Electrocardiogram) was first detected in 1895 by Willem Einthoven. During contraction, electrical impulses are spread through the muscles in the heart, which can be safely measured using an ECG machine.

An ECG is done:

- To track the heart rate,
- To pin-point the symptoms of shortness of breath, dizziness, fainting, palpitations and angina,
- To measure efficiency of the medicines and mechanical devices implanted in the heart,
- To monitor heart conditions of people with ancestral heart problems,
- To find the extent of hypertrophy in the heart muscle.

Principle of ECG: The cells in the heart muscle develops a negative charge called the membrane potential. Using depolarization technique, this negative charge can be decreased by the stream of Na+ and Ca++ ions resulting in the contraction of the cell. During each heartbeat, small electrical variations occur due to the depolarization of the heart muscle. These variations in voltage are detected by the ECG electrodes that are

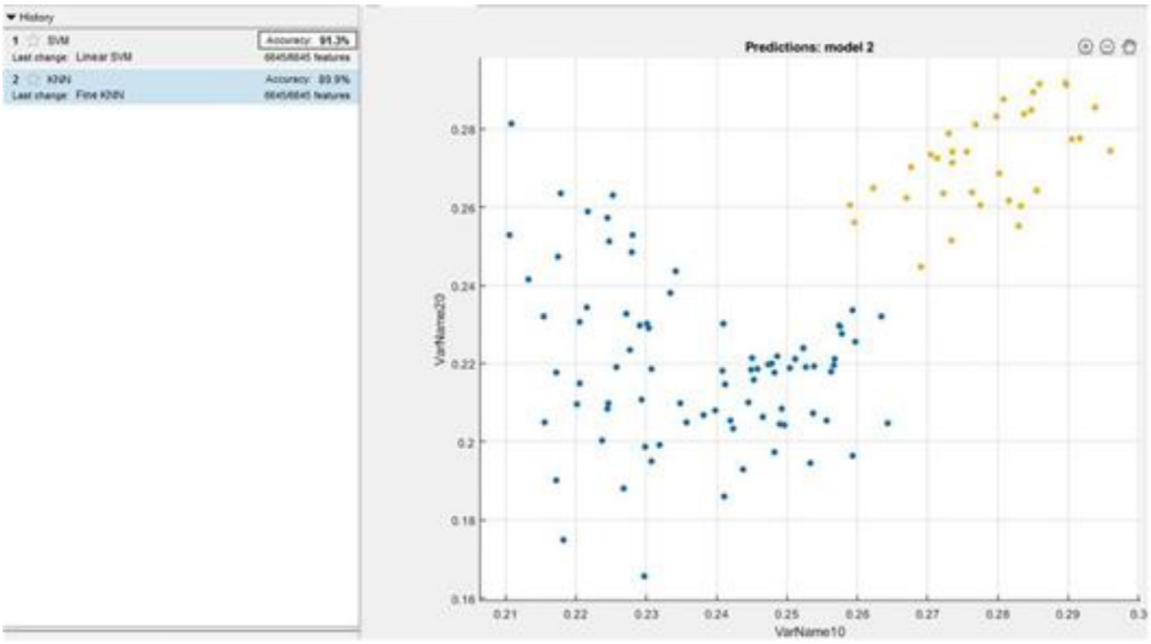

Fig. 1. Accuracy- SVM-91.3%, KNN-89.9% [43].

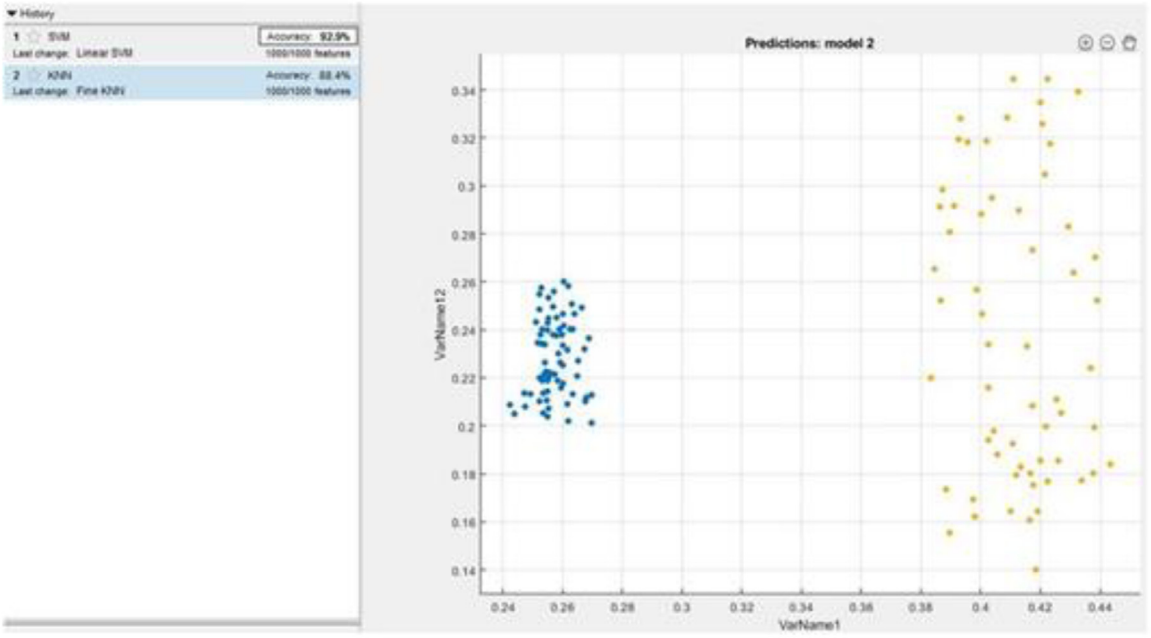

Fig. 2. Accuracy- SVM-92.9%, KNN-88.4% [43].

placed on the heart. These signals can be visualized on a display where wavy lines indicate the rhythm of the heart. These also indicate the weakness in different parts of the heart muscle.

The QRS complex, P wave, T wave, and U wave (hidden by T and P wave in approximately 50–75% of ECGs) can be visualized on the ECG display. The flat horizontal segment is measured with the tracing following the *T* wave and preceding the *P* wave. In a healthy heart, this baseline indicates the period when there are no currents towards the positive or negative ends of the ECG leads. It is equivalent to an isoelectric line which is 0 mV. However, in a diseased or unhealthy heart this baseline is either depressed or elevated to the isoelectric line.

During the ST segment there will be no current in the ECG leads as in this period the ventricles are fully depolarized. The baseline depression often appears as an elevation of ST segment, conversely the baseline elevation often appears as a depression of the ST segment. Fig. 4 shows the ECG waveform and Fig. 5 shows the real ECG signals.

The electrocardiographic depressions are labelled as:

- The P wave represents the Atrial contraction.
- QRS complex represents the Depolarization or Ventricular activation.
- T wave represents the Ventricular repolarization.
- ST segment, *T* wave and *U* wave represents the duration of ventricular recovery.

Important parameters:

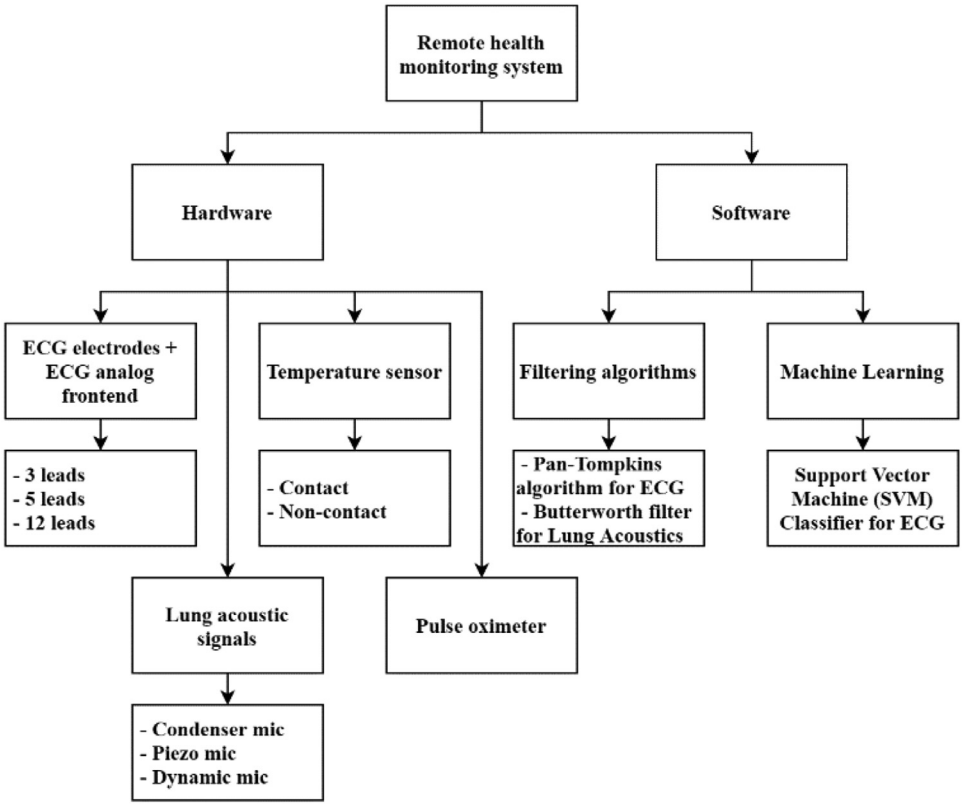

Fig. 3. Taxonomy of research.

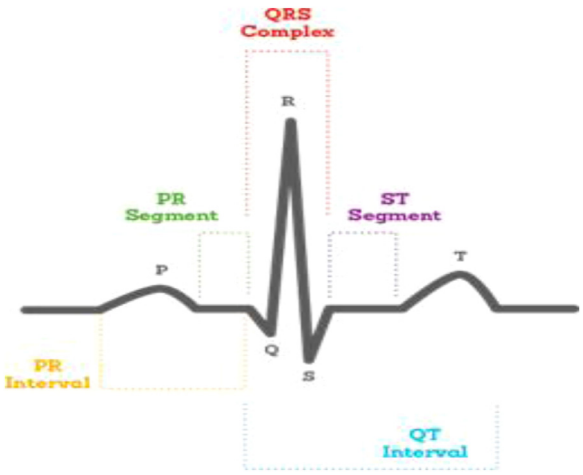

Fig. 4. ECG Waveform [44].

- RR interval – It is the interval between one *R* wave and the next *R* wave. Its duration is 0.6–1.2 s.
- PR interval – It is measured from the beginning of the *P* wave to the beginning of the QRS complex. It represents the time the electric impulse takes to travel from the SA node to the AV node and enter the ventricles. It is a good estimation of the AV node function. The duration of the PR interval is 120–200 ms.
- P wave – During the depolarization of the Atria, the electrical vector is directed from the SA node to the AV node and it spreads from right atrium to the left atrium. This represents the P wave on ECG. The duration of a *P* wave is less than 0.12 s.
- PR segment – It connects the P wave and the QRS complex. Here the impulse vector travels from the AV node to the Bundle of His and then to the Purkinje fibres. This does not produce a contraction hence this segment is flat on the ECG. The duration of the PR segment is 50–120 ms.
- QRS complex – It represents the depolarization of the right and left ventricles. The ventricles have greater muscle mass than atria, thus the complex has a larger amplitude. The duration of the QRS complex is less than 0.10 s.
- ST segment – It connects the QRS complex and the *T* wave. It represents the period of depolarization of ventricles. The duration of ST-segment is 80–120 ms.
- ST interval – It is measured from J-point to the end of *T* wave. The duration of the ST interval is 320 ms.
- QT interval – It is measured from the beginning of the QRS complex to the end of the *T* wave. When a QT interval is prolonged, it can result in sudden death. The duration of the QT interval in males is less than 0.45 s and in females, it is less than 0.45 s when the heart rate is 60 bpm.

Comparison between various ECG sensor leads – 3, 5 and 12 and their features is given in Table 2.

2.1.2. *ECG analog front-end*

The front end of the ECG deals with extremely weak signals. These signals can range from 0.5 to 5.0 mV, combined with ± 300 mV of dc component. These voltages are the results of the electrode-skin contact. And an additional 1.5 V of a common-mode component from the potential between electrodes and ground. The ECG bandwidth ranges from 0.5 to 50 Hz for monitoring intensive care units. Typically, the analog front end uses an instrumentation amplifier with a common-mode feedback op-amp. A comparison between various ECG analog frontend devices is shown in Table 3.

2.1.3. *Lung acoustics*

Lung acoustic sounds are the sounds produced due to the movement of air through the respiratory system. These sounds are identified

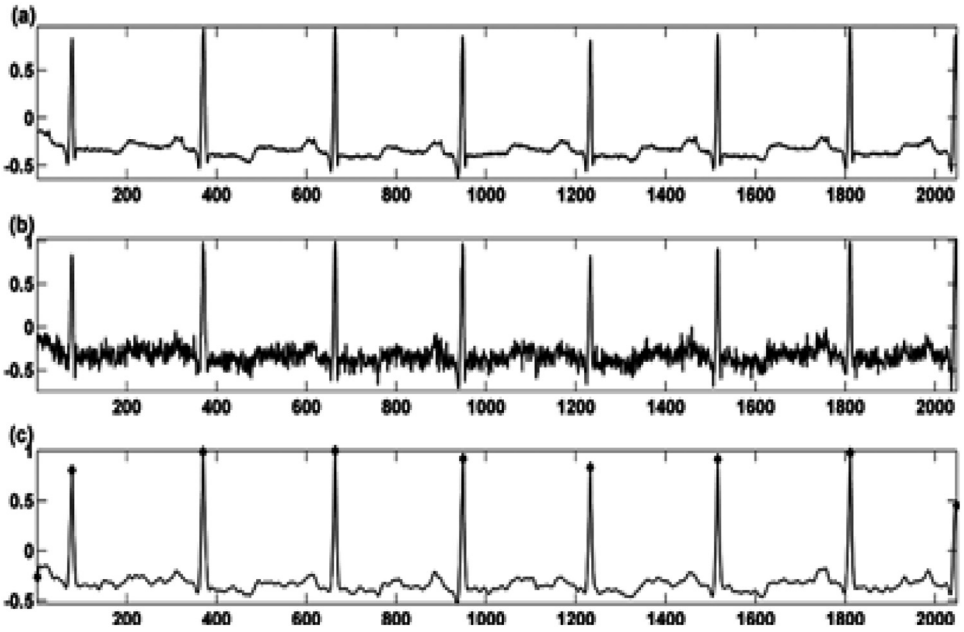

Fig. 5. Real ECG Signals [45].

Table 2
Comparison between 3-lead, 5-lead and 12-lead ECG electrodes [1].

ECG Type	Features
3-Lead ECG	Uses 3 electrodes on the torso Provides diagnostic information for most cardiac diseases Cost-efficient Convenient to use
5-Lead ECG	Uses 5 electrodes on the torso Correct placing of the electrode is crucial Poor electrode placement can result in misdiagnosis, misinterpretation
12-Lead ECG	Uses 10 electrodes on the torso and limbs Provides detailed information for prehospital diagnosis Not feasible and difficult to interpret. Limb movement, anxiety and cold extremities can interfere with ECG readings

through auscultation (using a stethoscope). These signals are very important in differentiating normal and abnormal lung sounds. There are two categories of lung sounds: Continuous and Interrupted (discontinuous).

From the comparison in Table 4, it is very clear that tracheobronchial sounds are a more widely accepted diagnostic aid in auscultation of lung sounds. These sounds are more pertinent in diagnosing different abnormal breath sounds based on their frequencies and amplitude.

2.1.4. Effect of COVID-19 on lung sounds

The outbreak of novel COVID-19 has a major impact, especially on lungs as they cause severe acute respiratory problems. Although in initial stages patients show fever and cold-like symptoms, at the later stages they are prone to various degrees of pulmonary abnormalities. These abnormalities become severe; it may result in the death of the infected people, thus increasing the mortality rate. According to the research done by various doctors and scientists, it is concluded that infected patients who have a medical history of any pulmonary abnormalities, diabetic

Table 3
Comparison between various ECG analog frontend devices [46,47].

Texas Instruments	Analog Devices
ADS1293 Low-Power, 3-Channel, 24-Bit Analog Front-End for Bio potential Measurements	ADAS1000-2 Low Power 5 electrode ECG Analog Front End Companion Chip
Features:	Features:
Three High-Resolution Digital ECG Channels with Simultaneous Pace Output	Bio potential signals in; digitized signals out
EMI-Hardened Inputs	5 acquisition (ECG) channels and one driven lead
Input-Referred Noise: 7 μVpp (40 Hz Bandwidth)	Parallel ICs for up to 10+ electrode measurements
Input Bias Current: 175 pA	Internal pace detection algorithm on 3 leads
Built-In Oscillator and Reference	Selectable reference lead
Battery Voltage Monitoring	Scalable noise vs. power control, power-down modes
Flexible Power-Down and Standby Modes.	Low power operation from 11, 15, to 21 mW
Low Power: 0.3 mW/channel	
Applications:	Applications:
Portable 1/2/3/5/6/7/8/12-Lead ECG	Life Sciences & Medical Instrumentation
Patient Vital Sign Monitoring	Vital Signs Measurements
Automated External Defibrillator	Electrocardiogram (ECG) Measurement
Sports and Fitness (Heart Rate and ECG)	Electroencephalogram (EEG) Measurement

Table 4
Comparison between Bronchial lung sound and vesicular lung sound [48].

Bronchial Lung Sound	Vesicular Lung sound
Origin: Between nasal cavity and principal bronchi.	Origin: Deep beneath the chest (solely in larynx).
Characterization: Hollow or tubular as it passes through pulmonary alveoli.	Characterization: Vesicles /Alveoli.
Tracheobronchial sounds are detected from about 100 Hz.	Vesicular breath sounds distinguishable at 100 Hz.
Amplitude increases in proportion to airflow rate over frequency range 100–800 Hz.	Amplitude falls off to baseline values around 900 or 1000 Hz.
Slowly declining between inspiration and expiration.	Rapid declination between inspiration and expiration.
Frequency maxima is higher during expiration.	Frequency maxima lower during expiration.

Table 5
Comparison between air-coupled and contact sensors based on dimensions [19].

Sensors	Height(mm)	Weight(gm)	Diameter(mm)
Air-coupled			
Sony ECM155	12.0	1.7	5.6
Sony ECM77	12.0	1.5	5.6
Radio Shack No33-1052	8.9	2.0	7.6
Contact			
HP21050	26.0	52.2	14.0
Seimens EMT25C	13.0	15.4	28.0
PPG No201	8.0	9.9	28.0
FYSPac2	5.1	2.1	20.0

Table 6
Comparison between air-coupled and contact sensors based on performance [19].

Sensors	**S/N**	**Slope**	**F_M**
Air-coupled			
Sony ECM155*	41.4	-25.2	1250
Sony ECM77*	42.2	-26.7	1010
Radio Shack No33–1052	38.6	-16.9	1370
Contact			
HP21050	42.0	-15.9	1610
Seimens EMT25C	33.0	-16.1	1560
PPG No201	41.1	-16.0	>2000
FYSPac2	40.3	-11.4	>2000

Table 7
Comparison between different microphones [1].

Factors	Weight	Microphone Type (Ratings)		
		Condenser Mic	Piezo Mic	Dynamic Mic
Size	0.25	6	2	5
Cost	0.40	9	3	4
Sensitivity/Fidelity	0.10	7	4	6
Simplicity	0.45	7	8	8
Total	1.0	8.5	4.40	5.50

patients and old aged people are more obvious to fall under the severe category causing death. Respiratory sound features of COVID-19 include bronchial breathing (pneumonia), stridor (upper airway obstruction), wheeze, rhonchus, cackles, and pleural friction rub.

Lung acoustic signals are assessed by subjective auscultation using microphones. Microphones play a vital role in the measurement of respiratory sounds.

From the comparisons in Tables 5 and 6, it is clear that air-coupled sensors are more efficient than contact sensors in the assessment of lung acoustic signals [52–55].

For auscultation of lung sounds, based on the literature survey the following sensors were considered:

- Condenser microphone, also called capacitor/electrostatic microphones, are made up of capacitors. The diaphragm acts as one of the plates and the vibrations are produced in between the plates.
- Piezo microphone, also called a contact microphone, which senses the audio vibrations that are in contact with the objects.
- Dynamic microphone, also called a moving-coil microphone works on the principle of electromagnetic induction. A small inductive coil is placed in the magnetic field of a permanent magnet [56–58].

Sensitivity is one of the most parameters to be considered for accurate results, as per the comparison shown in Table 7, it is seen that the condenser mic has the highest rating. Considering the cost of all the three sensors it is observed that condenser mic costs less comparatively.

2.2. Processing of lung acoustic signals

Lung sounds are amplified using audio amplifier as per the individual audio signal level. The amplified signals are filtered using Butterworth filters in the range 100–2000 Hz. These amplified signals are digitized using 12-bit ADC at frequency of 10 kHz.On these digitized data Fourier Transform is performed to obtain power spectral analysis of the acquired acoustic signal. Before spectral computation a tapering functional window i.e., Hanning window is preferred. The upper and lower limits of lung sounds are fixed such that it drops to less than 3 dB above background noise, the limit defined is around 200 Hz.

2.2.1. Temperature sensor

The degree of hotness or coldness in an object is measured using a temperature sensor. Temperature measurement is provided in a readable format using electrical signals. The construction of a basic temperature sensor includes two metals which generate electric voltage or resistance when it senses a temperature change. Temperature sensor consists of two physical types, Contact and non-contact temperature sensor –

2.2.1.1. Contact temperature sensor. This type of temperature sensor is required to be in physical contact with the object that is being sensed. Any temperature change is monitored using the principle of conduction. Few examples include a thermistor, thermostat, RTD (Resistive Temperature Detectors), and thermocouple. The characteristics of various contact temperature sensors is shown in Table 8.

2.2.1.2. Non-contact temperature sensor. In this case, the change in temperature is monitored using the principle of convection and radiation. Here, the thermal radiation emitted by the object is measured from a distance using the infrared sensor. Examples include thermal imaging and infrared sensors.

The advantages and disadvantages between different contact temperature sensors such as Thermocouples, Resistance Temperature Detector (RTD), Thermistors and IC sensors is tabulated in Table 9.

2.2.2. Pulse oximeter

Pulse oximetry is a non-invasive method to measure the oxygen saturation level in the blood. Even small changes in oxygen that are carried

Table 8
Characteristics table of various contact temperature sensors [49].

Characteristics	Thermocouple	RTD	Thermistor
Temperature range	-210–1700 ^{0}C	-240–650 ^{0}C	-40–250 ^{0}C
Linearity	Fair	Good	Poor
Sensitivity	Low	Medium	Very high
Response time	Medium to fast	Medium	Medium to fast
Stability	Fair	Good	Poor
Accuracy	Medium	High	Medium
Durability	Excellent	Good	Poor
Cost	Least	High	Low
Signal conditioning requirements	Cold-junction compensation Amplification Open thermocouple detection Scaling	Excitation Lead resistance correction Scaling	Excitation Scaling
Susceptible to self-heating	No	Yes, minimal	Yes, highly

Table 9
Advantages and Disadvantages between different Contact temperature sensor measurements [49].

Thermocouple	RTD	Thermistor	I.C. Sensor
Advantages			
Self-powered	Most stable	High output	Most linear
Simple and Rugged	Most accurate	Fast	Highest output
Inexpensive	More linear than thermocouple	Two-wire ohms measurement	Inexpensive
Wide temperature range			
Disadvantages			
Non-linear	Expensive	Non-linear	Power supply required
Low voltage	Current source required	Limited temperature range	Slow
Reference required	Low absolute resistance	Fragile	Self-heating
Least stable	Self-heating	Current source required	Limited configurations
Least sensitive			

throughout the entire body can be efficiently detected. The main purpose of pulse oximetry is to determine the wellness of the heart, and its oxygen pumping capability [50].

Health conditions that affect the blood oxygen levels are,

- COVID-19
- Chronic Obstructive Pulmonary Disease (COPD)
- Asthma
- Pneumonia
- Heart failure
- Congenital heart defects
- Lung cancer

Pulse oximeter is a non-invasive sensor which is a small, light-weight chip that can be clipped onto the fingertip. It uses the concept of measuring the changes of light absorption in the blood by sending beams of light to pass through the blood in a finger, to calculate the pulse rate amount of oxygen carried in the body.

Blood Oxygen Saturation (SpO2):

SpO2 reading gives an estimated amount of oxygen in the blood. For a normal oxygen level, the SpO2 reading should be 95% or higher. A reading of 92% or less suggests that the blood saturation in the body is poor.

Pulse rate:

The number of times the human heart contracts per minute is known as pulse rate. In adults, the normal pulse rate ranges from 60 to 100 beats per minute [51]. Any changes from this normal range indicate abnormal heart conditions.

Within seconds, the pulse oximeter gives accurate readings about the SpO2 and pulse rate. This advance in the sensor device made it very easy and helpful for at-home individual health monitoring. Factors such as body movements, nail polish, and color interferences cause an error in the pulse oximeter measurement.

2.3. Filtering algorithms

The obtained ECG output values contain noise. These signals are processed using the following algorithms,

2.3.1. Pan-Tompkins algorithm

Jiapu Pan and Willis. J. Tompkins proposed the Pan-Tompkins algorithm in 1985, in the journal IEEE Transactions on Biomedical Engineering. It is one of the most widely used algorithms to detect the QRS complexes in Electrocardiographic Signals (ECG). The main spike visible in an ECG signal, i.e., the ventricular depolarization is depicted by the QRS complex and is the main feature to assess the health condition of the heart. It is the first derivative-based algorithm. The algorithm identifies the R peaks in QRS complexes by using the amplitude, slope, and width of an integrated window.

The algorithm is implemented in two stages, pre-processing and decision. Noise removal, signal smoothing, width and QRS slope are increased in the preprocessing stage. In the decision stage, the noise peaks are eliminated by considering the signal peak thresholds. The algorithm consists of a band-pass filter, differentiation block, a squaring function, moving window integration, adaptive thresholds, and QRS complex detection block, as shown in the Fig. 6. The band-pass filter is used to increase efficiency as it cuts down the noise in the ECG signals. The thresholds are updated automatically with parameters to counter the changes in heart rate.

2.3.2. Support vector machine (SVM) classifier

SVM classifier is a supervised machine learning model that is used to classify a set of data into two groups. For the QRS detection, SVM is used to delineate or differentiate the QRS and non-QRS regions of an ECG signal. It uses the best hyperplane method for classification and can also classify non-linear data.

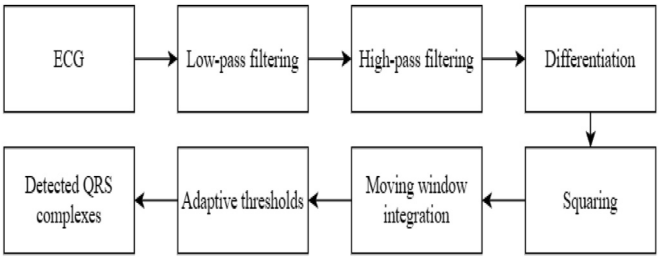

Fig. 6. Stages in Pan-Tompkins algorithm.

3. Conclusion

This paper takes into consideration the different parameters and methods that can be applied to tackle the current global health scenario. From the review of articles on ECG Signals, Lung acoustic signals, temperature sensor, and pulse oximeter it is clear that these factors can be used for diagnosis of COVID-19. A 3-Lead ECG has an edge over a 5 Lead and 12 Lead ECG as it is cost-efficient and is not difficult in designing and manufacturing. Features and applications' comparison of ECG frontend devices from Texas Instruments and Analog devices, types of contact and air-coupled microphones that can be used to measure lung acoustics are presented. Surveying different types of lung sounds, it is considered that tracheobronchial lung sounds are best for auscultation of lung acoustic signals. A detailed comparison of a condenser mic, piezo mic, and dynamic mic shows that condenser microphone is improved best for measuring lung acoustics signals because of its high sensitivity and low cost. After analyzing various temperature sensors, it is clear that non-contact infrared-based temperature sensors are the most optimal, since it does not require any contact with its user to measure their body temperature, thus reducing the risk of spreading coronavirus. The reviewed papers show that the Pan-Tompkins algorithm is one of the best algorithms to detect and characterize the QRS complex signals, with respect to other algorithms available. Research on classification algorithms indicates that SVM classifier is the most efficient and convenient to classify the ECG signals.

Declaration of Competing Interest

The authors declare that they have no known competing financial interests or personal relationships that could have appeared to influence the work reported in this paper.

Acknowledgment

The authors would like to express immense gratitude to their mentors Dr. B.G. Shivaleelavathi and Dr. Veeramma Yatnalli for their support and motivation, and to the institution JSS Academy of Technical Education for providing the platform for conducting this work.

References

[1] P.B. Ramachandra, E. Green, R. Rajashekar, W. Chen, O. Shiba, N. Yang and A. Kurian, "Chest discomfort aid," 2015.
[2] D. Sanders, L. Ungar, M.A. Eskander, A.H. Seto, Ambulatory ECG monitoring in the age of smartphones, Clevel. Clin. J. Med. (2019) 483–493.
[3] A. Gurung, C.G. Scrafford, J.M. Tielsch, O.S. Levine, W. Checkley, Computerized lung sound analysis as diagnostic aid for the detection of abnormal lung sounds: a systematic review and meta-analysis, Respir. Med. 105 (9) (2011) 1396–1403.
[4] M. Shabaan, K. Arshid, M. Yaqub, F. Jinchao, M.S. Zia, G.R. Boja, M. Iftikhar, U. Ghani, L.S. Ambati, R. Munir, Survey: smartphone-based assessment of cardiovascular diseases using ECG and PPG analysis, BMC Med. Inform. Decis. Mak. 20 (2020) 177, doi:10.1186/s12911-020-01199-7.
[5] P. Dherange, J. Lang, P. Qian, B. Oberfeld, W.H. Sauer, B. Koplan, U. Tedrow, Arrhythmias and COVID-19: a review, JACC Clin. Electrophysiol. 6 (9) (2020) 1193–1204.
[6] A. Aliverti, Wearable technology: role in respiratory health and disease, Breathe (Sheff) 2 (2017) 27–36, doi:10.1183/20734735.008417.
[7] H. Panwar, P. Gupta, M.K. Siddiqui, R. Morales-Menendez, V. Singh, Application of deep learning for fast detection of COVID-19 in X-rays using nCOVnet, Chaos Solitons Fractals 138 (2020).
[8] G. Moody, R. Mark, The impact of the MIT-BIH Arrhythmia Database, IEEE Engineering in Medicine and Biology Magazine 20 (2001) 45–50, doi:10.1109/51.932724.
[9] M.H. Fan, M.H. Guan, Q.C. Chen, L.H. Wang, Three-lead ECG detection system based on an analog front-end circuit ADS1293, in: Proceedings of the IEEE International Conference on Consumer Electronics - Taiwan (ICCE-TW), 2017.
[10] R.J. Oweis, E.W. Abdulhay, A. Khayal, A. Awad, An alternative respiratory sounds classification system utilizing artificial neural networks, Biomed. J. 38 (2015) 153–161, doi:10.4103/2319-4170.137773.
[11] A. Leal, R. Couceiro, I. Chouvarda, N. Maglaveras, J. Henriques, R. Paiva, P. Carvalho, C. Teixeira, Detection of different types of noise in lung sounds, Annu. Int. Conf. IEEE Eng. Med. Biol. Soc. (2016) 5977–5980, doi:10.1109/EMBC.2016.7592090.
[12] J. Kim, A.S. Campbell, B.E.F. d. Ávila, J. Wang, Wearable biosensors for healthcare monitoring, Nature Biotechnology 37 (2019) 389–406.
[13] M.M. Islam, S. Mahmud, L.J. Muhammad, M.R. Islam, S. Nooruddin, S.I. Ayon, Wearable technology to assist the patients infected with novel coronavirus (COVID-19), SN Comput. Sci. (2020).
[14] A.K. Joshi, A. Tomar, M. Tomar, A review paper on analysis of electrocardiograph (ECG) signal for the detection of arrhythmia abnormalities, Int. J. Adv. Res. Electr. Electron. Instrum. Eng. 2014 (2014) 12466–12475.
[15] A. Szczepański, K. Saeed, A. Ferscha, A new method for ECG signal feature extraction, in: Proceedings of the International Conference on Computer Vision and Graphics, 2010, pp. 334–341.
[16] Y. Li, X. Xu, Y. Liu, Y. Tian, Analysis and Implement of ECG Front-End Signal Processing Circuit," 2011 International Conference of Information Technology, Computer Engineering and Management Sciences (2011) 309–312, doi:10.1109/ICM.2011.131.
[17] F. Dalmay, M. Antonini, P. Marquet, R. Menier, Acoustic properties of the normal chest, Eur. Respir. J. 8 (10) (1995) 1761–1769, doi:10.1183/09031936.95.08101761.
[18] H. Pasterkamp, S. Patel, G.R. Wodicka, Asymmetry of Respiratory Sounds and Thoracic Transmission, Med. Biol. Eng. Comput. 35 (2) (1997) 103–106.
[19] H. Pasterkamp, S.S. Kraman, P.D. DeFrain, G.R. Wodicka, Measurement of respiratory acoustical signals. Comparison of sensors, Chest 104 (5) (1993) 1518–1525, doi:10.1378/chest.104.5.1518.
[20] M. Sarkar, I. Madabhavi, N. Niranjan, M. Dogra, Auscultation of the respiratory system, Ann. Thorac. Med. 10 (3) (2015) 158–168, doi:10.4103/1817-1737.160831.
[21] F. Meng, Y. Wang, Y. Shi, H. Zhao, A kind of integrated serial algorithms for noise reduction and characteristics expanding in respiratory sound, Int. J. Biol. Sci. 15 (9) (2019) 1921–1932, doi:10.7150/ijbs.33274.
[22] T.H. Falk, W.Y. Chan, Modulation filtering for heart and lung sound separation from breath sound recordings, Annu. Int. Conf. IEEE Eng. Med. Biol. Soc. 2008 (2008) 1859–1862, doi:10.1109/IEMBS.2008.4649547.
[23] N.S. Haider, R. Periyasamy, D. Joshi, B.K. Singh, Savitzky-Golay filter for denoising lung sound, Braz. Arch. Biol. Technol. 61 (4) (2018), doi:10.1590/1678-4324-2018180203.
[24] S. Nie, S. Han, H. Ouyang, Z. Zhang, Coronavirus disease 2019-related dyspnea cases difficult to interpret using chest computed tomography, Respir. Med. 167 (2020), doi:10.1016/j.rmed.2020.105951.
[25] S. Tian, W. Hu, L. Niu, H. Liu, H. Xu, S.Y. Xiao, Pulmonary Pathology of Early-Phase 2019 Novel Coronavirus (COVID-19) Pneumonia in Two Patients With Lung Cancer, J Thorac Oncol 15 (5) (2020) 700–704 Epub 2020 Feb 28. PMID: 32114094; PMCID: PMC7128866, doi:10.1016/j.jtho.2020.02.010.
[26] F.A. Padovani, T.H. Mcmains and M.R. Rowlette, "Temperature SENSOR". USA Patent 5,372,427, 1994.
[27] T.M. Betzner, D.P. O'Connell, P.J. Straub and M.J. Boehm, "Temperature sensor with flexible circuit substrate". USA Patent US 6,588,931 B2, 2003.
[28] H. Mansor, M.H.A. Shukor, S.S. Meskam, N.Q.A.M. Rusli, N.S. Zamery, Body temperature measurement for remote health monitoring system, 2013 IEEE International Conference on Smart Instrumentation, Measurement and Applications (ICSIMA), 2013, pp. 1–5, doi:10.1109/ICSIMA.2013.6717956.
[29] A.H. Kioumars, L. Tang, Wireless network for health monitoring: heart rate and temperature sensor, 2011 Fifth International Conference on Sensing Technology, 2011, pp. 362–369, doi:10.1109/ICSensT.2011.6137000.
[30] T.Q. Trung, S. Ramasundaram, B. Hwang, N. Lee, An all elastomeric transparent and stretchable temperature sensor for body attachable wearable electronics, Adv. Mater. 28 (3) (2015) 502–509, doi:10.1002/adma.201504441.
[31] A. Jubran, Pulse oximetry, Critical Care 3 (2015), doi:10.1186/cc341.
[32] M.J. Moron, E. Casilari, R. Luque, J.A. Gazquez, A wireless monitoring system for pulse-oximetry sensors, 2005 Systems Communications (ICW'05, ICHSN'05, ICMCS'05, SENET'05), 2005, pp. 79–84, doi:10.1109/ICW.2005.20.
[33] M. Nitzan, A. Romem, R. Koppel, Pulse oximetry: fundamentals and technology update, Med. Devices Evid. Res. 7 (2014) 231–239.
[34] A. Louie, J.R. Feiner, P.E. Bickler, L. Rhodes, Four Types of Pulse Oximeters Accurately Detect Hypoxia during Low Perfusion and Motion, Anesthesiology 128 (3) (2018) 520–530, doi:10.1097/ALN.0000000000002002.
[35] S. Seifi, A. Khatony, G. Moradi, A. Abdi, F. Najafi, Accuracy of pulse oximetry in detection of oxygen saturation in patients admitted to the intensive care unit of heart surgery: comparison of finger, toe, forehead and earlobe probes, BMC Nursing 17 (2018), doi:10.1186/s12912-018-0283-1.
[36] J. Pan, W.J. Tompkins, A real-time QRS detection algorithm, IEEE Trans. Biomed. Eng. BME-32 (1985) 230–236, doi:10.1109/TBME.1985.325532.
[37] Z. Fariha, R. Ikeura, S. Hayakawa, S. Tsutsum, Analysis of Pan-Tompkins algorithm

performance with noisy ECG signals, in: Proceedings of the 4th International Conference on Engineering Technology (ICET 2019), 1532, p. 2020. Conference Series.
[38] F. Liu, C. Liu, X. Jiang, Z. Zhang, Y. Zhang, J. Li, S. Wei, Performance analysis of ten common QRS detectors on different ECG application cases, J. Healthc. Eng. 2018 (2018), doi:10.1155/2018/9050812.
[39] R.A. Álvarez, A.J.M. Penín, X.A.V. Sobrino, A comparison of three QRS detection algorithms over a public database, Procedia Technol. 9 (2013) 1159–1165.
[40] S. Mehta, N. Lingaya, SVM-based algorithm for recognition Of QRS complexes in electrocardiogram, IRBM 29 (5) (2008) 310–317.
[41] G. Van, K. Podmasteryev, Algorithm for detection the QRS complexes based on support vector machines, Journal of Physics Conference Series 929 (2017) Saint-Petersburg, doi:10.1088/1742-6596/929/1/012041.
[42] B.M. Asl, S.K. Setarehdan, M. Mohebbi, Support vector machine-based arrhythmia classification using reduced features of heart rate variability signal, Artif. Intell. Med. 44 (1) (2008) 51–64.
[43] N. Vemishetty, R.L. Gunukula, A. Acharyya, P.E. Puddu, S. Das, K. Maharatna, Phase space reconstruction based CVD classifier using localized features, Sci. Rep. 9 (2019) 14593, doi:10.1038/s41598-019-51061-8.
[44] "What is an ECG?," AliveCor, [Online]. Available: https://www.alivecor.com/education/ecg.html.
[45] F. Eric, O. Laligant, B. Jalil, Signal restoration via a splitting approach, EURASIP J. Adv. Signal Process. 2012 (2012) 38, doi:10.1186/1687-6180-2012-38.
[46] "ADS1293 low-power, 3-channel, 24-bit analog front-end for biopotential measurements," December 2014. [Online]. Available: https://www.ti.com/lit/ds/symlink/ads1293.pdf?ts=1617710078731&ref_url=https%253A%252F%252Fwww.google.com%252F. [Accessed 2021].
[47] "ADAS1000-2 low power 5 electrode ECG analog front end companion chip," [Online]. Available: https://www.analog.com/en/products/adas1000-2.html#. [Accessed 2021].
[48] F. Dalmay, M.T. Antonini, P. Marquet, R. Menier, Acoustic properties of the normal chest, Eur. Respir. J. 8 (10) (1995) 1761–1769, doi:10.1183/09031936.95.08101761.
[49] "Overview of temperature sensors," NI, 2020. [Online]. Available: https://www.ni.com/en-in/innovations/white-papers/06/overview-of-temperature-sensors.html. [Accessed 2021].
[50] L.J.L. Sujan, V.D. Telagadi, C.G. Raghavendra, B.M.J. Srujan, R.V. Prasad, B.D. Parameshachari, K.L. Hemalatha, Joint reduction of sidelobe and PMEPR in multicarrier radar signal, in: Cognitive Informatics and Soft Computing, Springer, Singapore, 2021, pp. 457–464.
[51] P. Subramani, K. Srinivas, R. Sujatha, B.D. Parameshachari, Prediction of muscular paralysis disease based on hybrid feature extraction with machine learning technique for COVID-19 and post-COVID-19 patients, Pers. Ubiquitous Comput. (2021) 1–14, doi:10.1007/s00779-021-01531-6.
[52] S.I. Chu, C.L. Wu, T.N. Nguyen, B.H. Liu, Polynomial computation using unipolar stochastic logic and correlation technique, IEEE Trans. Comput. (2021), doi:10.1109/TC.2021.3085120.
[53] K. Seyhan, T.N. Nguyen, S. Akleylek, K. Cengiz, S.H. Islam, Bi-GISIS KE: modified key exchange protocol with reusable keys for IoT security, J. Inf. Secur. Appl. 58 (2021) 102788.
[54] P. Kiran, B.D. Parameshachari, J. Yashwanth, K.N. Bharath, Offline signature recognition using image processing techniques and back propagation neuron network system, SN Comput. Sci. 2 (3) (2021) 1–8 196.
[55] W.B. Kannel, C. Kannel, R.S. Paffenbarger, L.A. Cupples, Heart rate and cardiovascular mortality: the Framingham study, Am Heart J. 113 (6) (1987) 1489–1494, doi:10.1016/0002-8703(87)90666-1.
[56] B.D. Parameshachari, Logistic sine map (LSM) based partial image encryption, in: Proceedings of the National Computing Colleges Conference (NCCC), IEEE, 2021, pp. 1–6.
[57] G. Chandrasekaran, T.N. Nguyen, D.J. Hemanth, Multimodal sentimental analysis for social media applications: a comprehensive review, Wiley Interdiscip. Rev. Data Min. Knowl. Discov. 11 (5) (2021), doi:10.1002/widm.1415.
[58] K. Yu, L. Tan, L. Lin, X. Cheng, Z. Yi, T. Sato, Deep-learning-empowered breast cancer auxiliary diagnosis for 5GB remote E-health, IEEE Wirel. Commun. 28 (3) (2021) 54–61 June.